ISSN: 2634-9221
European Journal of Applied Sciences; Vol. 14 No. 06 (2026) (142-160)
https://doi.org/10.14738/ejas.1406.12612

Identifying Gram-positive and Gram-negative Pathogenic Bacteria using Fourier Transform IR Spectroscopy and Principal Component Analysis

Javier C. Ramirez-Perez

1. Institute of Physics, Sao Paulo University, Rua do Matao 1371, Sao Paulo 05508-090, Brazil
2. Department of Chemistry, Kent State University at Stark, 6000 Frank Ave NW, North Canton, OH 44720, USA

Abstract: Parasitoids may compete at the adult stage when foraging hosts (extrinsic competition), or at the larval stage, when supernumerary parasitoids develop in the same host (intrinsic competition).A study including lepidopteran pest *Spodoptera littoralis* and novel (*Cotesia marginiventris*) and extant (*Microplitis rufiventris*) hymenopteran endoparasitoids, was carried out to investigate the effect of single and double parasitism at ovipotion times of 2hr and 48hr on endo-development of the wasps and competitive interactions between the parasitoid larvae. No significant differences in the endo-development time of the wasps were found between single or superparasitised hosts. Multiple parasitism increased the endo developmental time of both wasps. Singly parasitized hosts by *M. rufiventris* produced more wasps than those of *C. marginiventris*. Also, the percentage of emergence success by superparasitized *M. rufiventris*, was, greater than those recorded by superparasitized *C. marginiventris*. Muliparasitized hosts produced more *C. marginiventris* than *M. rufiventris* wasps. However, the outcome of competition, by both wasp larvae principally depended on the wasp species that was first to attack and on the time interval between two oviposition's by wasp females. The intrinsic and competitive interactions between the parasitoid larvae in multiple parasitism experiments was more frequently than in superparasitism experiments. The novel parasitoid, *C. marginiventris* was intrinsically superior competitor comparing with the extant *M. rufiventris*, so the use of the two species simultaneously may lead to competitive exclusion and influence the stability of the extant parasitoid population. The competition was asymmetrical, meaning one species (the exotic) had a competitive advantage as competitor being the victor whatever the sequence of attack, over the other species. Introducing *C. marginiventris* to Egypt, is not a good option for biological control of both, the new invasive pest, *S. frugiperda* and local one, *S. littoralis*.

Keywords: *Cotesia marginiventris, Microplitis rufiventris, Spodoptera littoralis*, single and double parasitism, endo-development, intrinsic competition

INTRODUCTION

Foodborne pathogen identification is becoming increasingly crucial in microbiological food safety. *Staphylococcus aureus, Escherichia coli, Salamonella spp, and Bacillus subtilis* are the most significant foodborne illness outbreaks resulting from the consumption of foods contaminated by bacterial toxins. *E.coli* consists of Gram-negative pathogen, some clinical symptoms of the illness include vomiting and diarrhea, hemorrhagic colitis and hemolytic uraemic syndrome, a cause of renal failure due to blood clots in the kidney tubules, and internal bleeding due to lack of blood platelets resulting in brain damage that can occur in

serious cases, which can lead to long-term complications and death. *Salmonella spp*. are Gram-negative and the most prevalent foodborne pathogens around the world and it is estimated that these microorganisms are responsible for approximately 1.35 million illnesses, 26,500 hospitalizations, and 420 deaths of food-transmitted salmonellosis annually only in the United States[1].

Staphylococcus aureus is an important Gram-positive pathogen that can cause serious infections in human such as pneumonia and bactermia and hospital-acquired infections worldwide. It is also responsible for approximately 1.1 million deaths worldwide each year,[2,3] and is the leading cause of bacterial sepsis in both developed and developing countries. The species can cause food poisoning and were responsible for most of the foodborne illness outbreaks resulting from the consumption of foods contaminated by staphylococcal toxins. The species *Bacillus subtilis* is a Gram-positive, it is rod shaped, endospore forming bacteria that are member of the phylum firmicutes. Owing largely to the fact that they are common inhabitants of soil and aquatic sediments, species within the species are widespread in nature and are found in virtually every environment. While their main roles appear to involve carbon and nitrogen cycling, some species are well known human and livestock pathogens and insect pathogens.[3]

Bacterial species are divided into two groups based on the characteristics of their cell walls. The cytoplasmic membrane of Gram-positive bacteria is covered by a thick cell wall made of peptidoglycans and teichoic acids (TAs), whereas the membranes of Gram-negative bacteria are separated by a thin layer of peptidoglycans.[4] Proteins, phospholipids, and lipopolysaccharides make up the outer membrane of Gram-negative bacteria. The outer membrane of Gram-negative bacteria is composed of proteins, phospholipids, and lipopolysaccharides. For example, in *Escherichia coli*, 80% of the peptidoglycan is present as a monolayer, and the overall thickness of the cell wall could exceed 4 nm.[5, 6] In contrast, Gram-positive bacteria such as *Staphylococcus aureus* lack an outer membrane and instead have a dense peptidoglycan component with multi layers.[4] Peptidoglycan is a polymer composed of glycan strands. It is formed from disaccharide residues cross-linked with amino acids.[4, 6] Furthermore, Teichoic Acids (TAs) are also found in the cell walls of Gram-positive bacteria but not in Gram-negative bacteria. TAs are glycerol phosphate-containing anionic polymers that are linked to the peptidoglycan layer or to the membrane's lipids (and appear as lipoteichoic acid, or LTA). The peptidoglycan layer of the bacterial cell wall, in particular, is a dynamic structure with numerous roles in preserving cellular shape and ensuring cell survival.[2,6]

Currently, various methods have been proposed for the detection and identification of these pathogenic bacteria are generally carried out using traditional methods based on biochemical or serological tests and molecular methods based on DNA/RNA, PCR assays and diagnostic marker analysis fingerprints.[7-9] However these methods are time consuming, labor intensive, considerable technical expertise are still limited for applicability in the routine laboratories. Biochemistry and biomedicine both employ spectroscopic methods more frequently. Infrared spectroscopy, Raman-SERS spectroscopy, and mass spectrometry are examples of these technologies as diagnostic tools that offer accurate ways to examine microorganisms.[10-14]

FTIR spectroscopy technique is a non-destructive, non -invasive analysis, high S/N (signal to noise ratio), label free, and cost-effective tool for studying molecular composition

and dynamics.[10, 11] In the case of microbial samples, the IR spectrum is a composite of the IR vibrations associated with literally thousands of molecular components in the microbe. These molecular components (e.g. fatty acids, intracellular and membrane proteins, polysaccharides, nucleic acids, and phospholipids) are common to all materials of biological origin and result in composite spectra consisting of few features and peaks since the bonds and functional groups of a particular molecular structure are often adequately peculiar as those associated with their pure biochemical compounds to afford a relatively simple, unique, and reliable spectral fingerprint, this behavior could be used for accurate classification of bacteria, even in the isolate level.[15- 17]. Therefore, FTIR is a potential method for rapid discrimination, classification and identification of pathogenic bacteria.[2, 20]

Moreover, statistical treatment of spectral data, powerful new algorithms for multivariate statistical analysis such as principal component analysis (PCA) and pattern recognition methodologies demonstrates that IR spectra can be used for discrimination between different pathogenic bacteria species.[18,19] Thus, the development of quick and accurate techniques to selectively distinguish pathogenic bacteria from other bacterial species in a variety of food products is required. The aim of this work was to use PCA analysis of IR spectra of four representative bacterial species including: *Escherichia coli*, *Salmonella ssp.*, *Staphylococcus aureus* and *Bacillus subtilis* based on spectral bands originating mainly from the cell wall materials, provided the primary bases for the discrimination of Gram-positive from Gram-negative bacteria, using the Brazilian Synchrotron Light Laboratory (LNLS) microscopy FTIR.

EXPERIMENTAL

Grow Conditions and Sample Preparation

All the pathogenic bacteria used in the present study come from specie collections at the Microbial Ecology and Biotechnology Laboratory at Federal University of Ceara-Brazil including: *Salmonella ssp* (ATCC 9270), and *E.coli* (ATCC 25922) as Gram-negative; *Staphylococcus aureus* (ATCC 25923) and *Bacillus subtilis* (ATCC 6633) as Gram-positive (Table 1). The species selected in this study were from specie collections, selected species were grown on the same media to avoid the influence of the grown medium on spectral similarity. All bacterial species had been kept frozen (–80 °C) containing 15% glycerol, before preparation. The stored bacterial species were sub-cultured and grown in Luria broth medium (Difco^{TM}) at 37±2 °C for 24 h. After the incubation period, the bacteria were ready by collecting the biomass from the surface of each plate using sterile inoculation loops and re-suspending in 1 mL of deionized water. Each sample of the examined bacteria was pelleted from the bacterium-containing media by centrifugation at 1000 rpm for 5 minutes, to eliminate the medium of any remaining particles. The concentration of bacteria was adjusted to achieve an optical density of 15 (OD 600) of approximately $6x10^5$/µl. For FTIR testing a 2 µl aliquot of each washed bacterial cells deposited onto a CaF_2 glass slide, which is transparent to IR radiation. Let the sample to form a thin dried film for about 10 minutes at room temperature before examined by FTIR analysis.[14, 17]

Table 1: Specific details of the tested bacterial species utilized in this investigation

Bacterial species selected*	No. of measured pure samples
Staphylococcus aureus	18
Salmonella spp.	18
Bacillus subtilis	18
Escherichia coli	18

* Three replicates of each bacterial specie were used to take six measurements on each sample at random locations

FTIR Micro-spectrometer

All the bacterial spectra were recorded in reflectance mode using an FTIR micro-spectrometer Agilent 670 including an IR microscope Agilent 620 set up with 32 x Schwarzschild objective (N.A.=0,65) at the LNLS. The FTIR micro-spectroscopy include a regular thermal source as illumination, LN_2 (liquid nitrogen cooled) MCT /FPC (focal plane array) detector(s), consisting of an array of infrared detector elements, that enables not only to collect the IR absorption spectrum of the sample, but also an IR chemical image contrast is given by the response of selected sample regions to particular IR wavenumbers. For each single-species culture analyzed, FTIR spectral measurements were obtained from at least 18 distinct locations (n=18) within each sample. This total comprised six spectra acquired across three analytical replicates to ensure intra sample reproducibility, encompassing the mid-IR region from 4000-550 cm^{-1}, with an average of 32 scans and 8 cm^{-1} spectral resolution. FTIR data were saved in log (1/R) format. The experiments were repeated three times over the course of the experimental investigation. No further processing data (smoothing, Fourier self-deconvolution, etc) was employed, to avoid the introduction of artifacts.[13, 17] Spectra are shown in log (1/R) format, the equivalent of absorbance for reflectance spectra, presented on the same scale within each group, and offset vertically for clarity.

Data Analysis

The results were presented as mean +/- standard deviation values. Using the R software and the Tukey test, the differences between the means of Gram-positive and Gram-negative bacteria were compared. Significant results were considered as a p-value ($p<0.05$*, $p<0.01$**). [13,15] In this study, PCA was employed to examine the FTIR spectra of the four bacterial species. The analysis enables us to investigate spectral data variations and determine the most significant effects to the variance taken into account by the principal components (PCs) as clustering algorithm. To assess the spectrum differences between the four distinct bacterial species under study and to distinguish between Gram-positive and Gram-negative bacteria, PCA was conducted on the pre-processed FTIR spectra. Before PCA and PCs spectra were submitted to baseline correction, smoothed via a Savitzky-Golay (SG) filter using an asymmetric least square PCA analysis, and vector normalization.[16]

The second derivative of four bacterial species was calculated using the SG algorithm for 25 smoothing points in the 550-1700 cm^{-1} wavenumber region. Data pretreatment, analysis, and presentation were performed using OriginPro 2018. 64 bit software.

RESULTS AND DISCUSSION

Infrared Absorption Spectra of the Four Bacterial Species Selected

It is well known that FTIR spectroscopy can be used to characterize a wide variety of biological samples in relation to their chemical composition. IR spectroscopy has become a promising tool for bacterial research over the past ten years. As one of the few methods that enables for phenotypic characterization through chemical composition, it continues to attract significant interest in the area of microbiology.

The representative, unprocessed FTIR spectra within the 4000–800 cm^{-1} spectral region, alongside high-resolution images of *Staphylococcus aureus*, *Escherichia coli*, *Bacillus subtilis*, and *Salmonella* spp.species are exhibited in Fig.1. This spectroscopic approach demonstrated high repeatability across all three dimensions, despite the presence of significant spectral overlap (Fig. S1†). The methodology successfully identified the fundamental vibrational bands of the major macromolecular compounds found in biological materials, including proteins, lipids, nucleic acids, carbohydrates, and other organic constituents. The assignments that have been proposed for these FTIR peaks are detailed in Table 2, and they are illustrated in Fig.2.

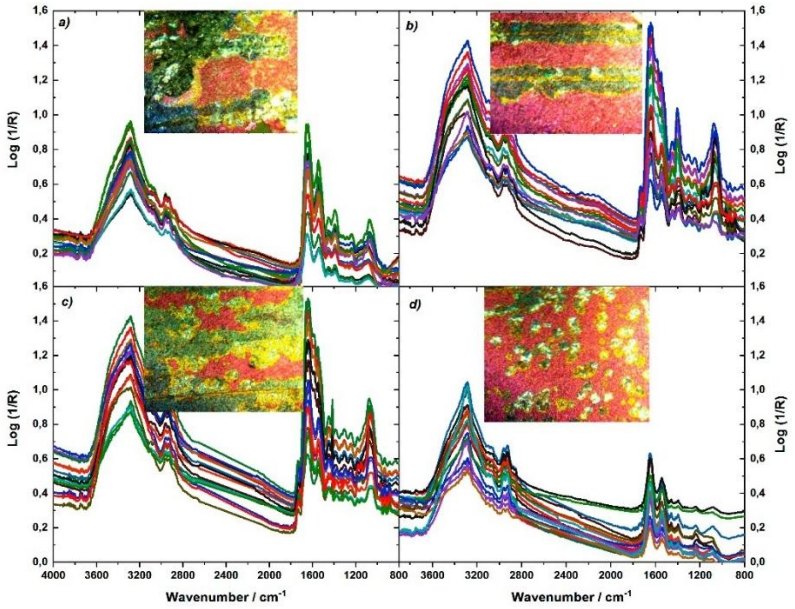

Fig. 1: FTIR raw spectra collected from representative Gram-positive and Gram-negative bacterial species and inset images of a) *Staphylococcus aureus*, b) *Bacillus subtilis*, c) *Escherichia coli*. and d) *Salmonella spp*. Spectra are shown in log (1/R) format, the equivalent of absorbance for reflectance spectra, Absorbance (vertical axis) displays on the same scale within each group. Horizontal axis displays wavenumbers (inverse wavelength) between 4000 and 500 cm^{-1}. High-resolution imaging of Gram-positive and Gram-negative Bacterial Species. Scale bar 2 µm at a spatial resolution of 0.8 nm/pixel.

The FTIR spectra of the four bacterial species are complex and can be divided into two highly sensitive spectral regions (Fig. 2): the first spanning 3800–2800 cm^{-1} and the second encompassing 1750–500 cm^{-1}. Most of the vibrational bands in both regions are

associated with macromolecular backbone conformation; each specific frequency corresponds to a distinct structural component. The first spectral region is primarily composed of proteins, phospholipids, and long-chain fatty acids because of the functional group's CH_2 and CH_3 symmetric and anti-symmetric stretching vibrations (Table S1†). Despite being processed as dried biofilms, the samples exhibited residual water content, both intracellular and extracellular.[20,21] Furthermore, the 1700–550 cm^{-1} region encompasses the complete biomolecular profile of cellular structures, including the cell wall, cytoplasm, and nucleic acids. However, no vibrational signals were shown for any of the bacterial species between 2800 and 1750 cm^{-1} (Fig.3).

Table 2: Major IR spectral bands observed in *S.aureus*, *B. subtilis*, *E.coli* and *Salmonella spp.*[7, 8, 10, 16, 20, 27, 30]

Wavenumber (cm^{-1})						Tentative assignments
Gram-positive		Gram-negative				
S. aereus	*B.subtilis*	Average.	*E.coli*	*Salm spp.*	Average.	
3300	3292	3296	3298	3290	3294	υ (N-H) amide A in proteins, and OH stretching vibration:polysaccharides
2971	2971	2971	2968	2971	2970	C-H υ_{as} of $>CH_2$, $>CH_3$ asymmetric stretch: methyl groups in fatty acids
2931	2928	2930	2926	2929	2928	CH_2 asymmetric stretch: methylene groups in fatty acids
2872	2868	2870	2868	2881	2875	CH_3 symmetric stretch: methyl groups in fatty acids
2852	2850	2851	2850	2852	2851	CH_2 symmetric stretch: methylene groups in fatty acids
1748	1738	1743	1742	1748	1745	> υ (C=O) of lipid esters, triglycerides
1645	1643	1644	1645	1648	1647	Amide I of α-helical and ß-plated sheet structures of proteins
1539	1537	1538	1539	1538	1539	Amide II bands of proteins
1388	1398	1393	1383	1394	1389	Amide III, C=O υ_s of COO- group in amino-acids, fatty acids
1233	1244	1239	1242	1231	1237	υ_{as} (P=O) of > PO_2^- phosphodiesters in phospholipids
1092	1060	1076	1060	1092	1076	υ_s (P=O) of $>PO_2^-$ in DNA, RNA, phospholipids, and TAs, LTAs
914	910	912	964	946	955	C-O-C ring deoxyribose, N^+-C stretch, nucleic acids
839	851	845	815	833	824	ρ (C-H) of $>CH_2$ of fatty acids, ´proteins
767	753	760	725	739	732	ρ (C-H) of $>CH_2$
638	642	640	676,00	690	683	C-C twist mode of Phe; G,T (ring breathing modes of DNA/RNA bases)e
560	570	565	573,00	567	570	δ(CCC) ring deformation, δ(COC) glycosidic linkage, Exocyclic deformation (saccharides)

υ, stretching; δ, bending; ρ, rocking, twist, twisting; s, symmetrical; as, asymmetrical; A, adenine; G, guanine;T, tyrosine; Phe, Phenylalanine.

Comparison of Gram-positive and Gram-negative Bacterial Species

Fig.3 displays the average FTIR spectra of the examined gram-positive and gram-negative bacterial strains in the 3800-2800 cm^{-1} region. Table 2 shows the complete lists of identified FTIR bands along with tentative peak assignments.[2,7] The broad and prominent band between 3296 cm^{-1} (Gram-positive) and 3294 cm^{-1} (Gram-negative) in the selected bacteria respectively, corresponds to the absorption due to stretching of N–H bands of amide in proteins.[23] The bands centered at 2939 cm^{-1} and 2851 cm^{-1} are the stretching modes of the symmetric and asymmetric CH_2 vibrations caused by the methylene groups in fatty acids, respectively.[24] Whereas the bands with centers at 2970 cm^{-1} and 2872 cm^{-1} is the stretching mode of symmetric and asymmetric CH_3 vibrations due to methyl groups in fatty acids.[23] Table S1† lists the frequency, intensity, full width at half maximum (FWHM), and values for both Gram-positive and Gram- negative selected bacteria.

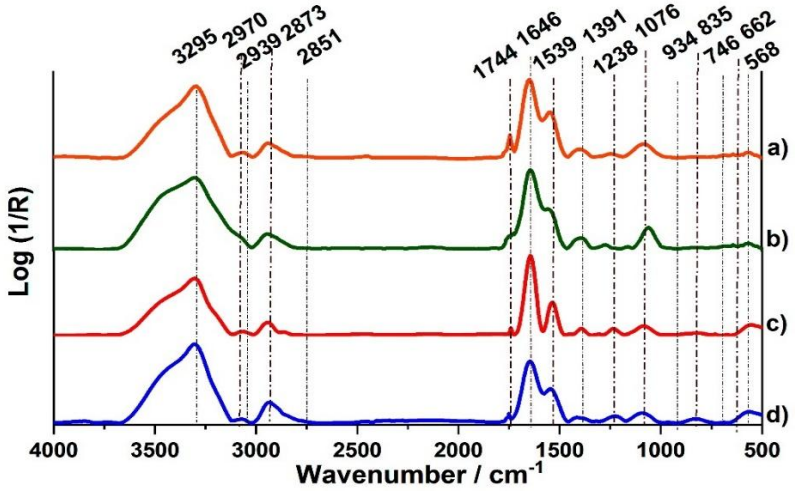

Fig. 2: Average FTIR spectral characteristics obtained from selected gram-positive and gram-negative bacteria in the 4000-500 cm^{-1} region: a) *S. aureus* (in orange), b) *B. subtilis* (in green), c) *Ecoli* (in red) and d) *Salmonella spp* (in blue) together with the most prominent bands labelled. Each FTIR spectrum was averaged from 54 tests recorded on random location on each bacterium sample. All FTIR spectra were baseline corrected, normalized and shifted vertically for improved visualization.

According to the table, Gram-negative bacteria (2969.31±0.00) cm^{-1} had a wavenumber of the CH_3 asymmetric stretching vibration was significantly lower than Gram-positive bacteria (2971.37±0.15) cm^{-1} ($p<0.05$). In addition, the absorption intensity of this band was significantly higher for Gram-negative bacteria (0.71±0.15) compared to Gram-positive bacteria (0.49±0.07) ($p<0.05$). Similarly, the absorption intensity of the CH_2 asymmetric stretching band was higher for Gram-negative (0,76±0.16) than for the Gram-positive bacteria (0.49±0.07). The wavenumber of the CH_3 symmetric stretching band is significantly higher (2874.63±0.02) cm^{-1} for Gram-negative than Gram-positive bacterial species (2870.01±0.15) cm^{-1}. Furthermore, Gram-negative bacteria have a higher intensity (0.73±0.15) than Gram-positive bacteria (0.41±0.09). Another observation was that both bacterial species exhibited a similar value in the intensity band (2851.24±0.03) cm^{-1} and (2851.34±0.04) cm^{-1} assigned as CH_2 symmetric stretching, indicating an equal number of gauche conformers, such as a similar in disorder status of the acyl chains.[24,25]

The signal strength and, more precisely, the full width at half-maximum (FWHM) area beneath peaks provide details regarding the concentration of the functional groups in responsible of the corresponding band.[20,24] A precise protein to lipid ratio can be determined from the FTIR spectrum by dividing the areas of the bands originating from lipids and proteins, whose concentrations in the membranes constitute a significant influence on the dynamics and structure of the membrane.[23,26] As can be seen from Table S2†, the ratio of protein to lipid can be calculated by summing the FWHM areas of the symmetric and asymmetric CH_2 and CH_3 bands in the 3000-2800 cm^{-1} region to the FWHM areas of amide I and amide II. This ratio was significantly lower ($p<0.01$) for the Gram negative (0.75±0.14) than for the Gram-positive selected bacteria group (0.82±0.03).

The band centered at 1744 cm^{-1} band is attributed to the ester >C=O ester stretching vibration of lipids which are abundant in cell membranes, such as cholesterol, phospholipids,

and triglycerides. As illustrated in Fig. 3, the average FTIR spectrum of *Staphylococcus aureus* shows a weak band at 1748 cm^{-1} but higher than in case of *Escherichia coli* (1742 cm^{-1}). Despite the lack of an outer membrane in Gram-positive cell walls which result in lower content of lipoproteins and phospholipids, Gram-negative bacteria have an outer cell membrane that is rich in lipoplysacharides and phospholipids, resulting in a higher total lipid content of their cell wall. As a result,–the cell wall of Gram-negative bacteria has a higher total lipid content. Thus, peptidoglycans and TA (Teichoic Acid) especially lipoteichoic acid (LTA), may be responsible for the intense carbonyl mode observed in the spectra of *Staphylococcus aureus*. It could be responsible for the Gram-positive cell wall signals at the band centered at 1745 cm^{-1}.[16, 20, 22]

Within the second spectral region, the four bacterial species exhibited significant differences in their FTIR spectra and their corresponding second derivatives. These variations were particularly pronounced in the 1700–550 cm^{-1} interval (Fig. 4). The amide region of proteins, which comprises amide I and II variants, is predominantly reflected by the bands centered at 1646 cm^{-1} corresponding to the stretching C=O and bending C-N (amide I) vibrational modes of the polypeptide and protein backbone. The band at 1539 cm^{-1} is assigned to the bending N-H and stretching C-N (amide II).[22,24,27] The amide I vibration, peaking between 1644-1690 cm^{-1} arises mainly from the C=O stretching vibration from peptide bonds in proteins. This band is composed of the superposition of sub-bands associated with the secondary structure of proteins like α-helices (1656 cm^{-1}) and ß-sheets (1637 cm^{-1}).[28, 29] In spectral data from bacteria, the signal intensity obtained from α-helices is usually superior than the signal collected from ß-sheets, hence, amide I band is centered around 1646 cm^{-1} due to the proximity of both peaks. Second derivatives are usually the preferred option to assess overlapped bands, in such cases, strong α-helices modes (1647 cm^{-1}) and ß-sheets (1644 cm^{-1}) is evident in the second derivatives of the FTIR spectra of Gram-negative and Gram-positive bacteria, respectively, which could indicate a major protein contribution to the FTIR spectrum of the cell wall and cytoplasm. The Gram-positive group has lower frequency value for the amide I band than the Gram-positive group, as shown in Fig. 3 and Table S1†. In addition, the intensity of amide I was higher ($p<0.05$) in the Gram-positive group (0.85±0.21) than in the Gram-negative group (0.70±0.18), the signal intensity obtained from α-helices in spectral data from bacteria is typically, greater than the signal acquired from ß-sheet, these discrepancies may be related to the amount of material tested by each specie. Both Gram positive and Gram-negative bacteria species coincidentally achieve the absorbance bandwidth of the amide II centered at 1539 cm^{-1}. The intensity is also greater for Gram-positive bacteria (0.68±0.19) than for Gram-negative bacteria (0.56±0.17) ($p<0.05$) at 1539 cm^{-1} due to the interaction between N-H vibration with C-N stretching from peptide groups [30], which corresponds to the contributions of the peptide bond group (amide II) combined δ(N–H) and ν(C–N), according to another study.[26] This is true even when comparing the spectra of amide I and amide II with those from our own study, this also reveals an important protein contribution to the IR spectrum of the cell wall and cytoplasm of Gram-positive bacteria.

The band centered at 1391 cm^{-1} is attributed to COO^- symmetric stretching vibrations of amino acid side chains and fatty acids [20, 27, 16]. The COO^- symmetric stretching vibration band at 1393 cm^{-1} had a greater intensity in the Gram-positive spectrum (0.48±0.85) than the Gram-negative spectrum (0.34±0.08), ($p<0.05$). The frequency of this band was also much lower for Gram-positive (1388.46 ±0.42) than Gram-negative (1393.83 ±0.49), ($p<0.05$)

(Table 1S†). Both the medium strong at 1076 cm^{-1} and the weak band centered at 1238 cm^{-1} are mainly caused by the asymmetric and symmetric stretching modes of phosphodiester groups, which are found in a variety of chemical components including nuclei acids, DNA, phospholipids originating from phosphate-containing substances in the cell wall including peptidoglycan and TA, LTA.[16, 27, 28] Analysis of these bands showed that the infrared spectra of Gram-positive and Gram-negative bacteria differed significantly. The bands (1076 and 1238 cm^{-1}) that were easily discernible in the spectra of *Staphylococcus aureus* and *Bacillus subtilis* were significantly weaker (or absent) in the spectra of *Escherichia coli* and *Salmonella spp*. These bands were associated to complex sugar modes of cell wall-related compounds, such as the peptidoglycan layer.[16, 27, 31] Gram-positive bacteria (1238.72±0.51 cm^{-1}; 0.35±0.02) were significantly higher ($p<0.05$) than Gram-negative bacteria (1236.49 ±1.35 cm-1; 0.31±0.07) in frequency and intensity of the phosphate asymmetric stretching band. In addition, the frequency and intensity of the phosphate symmetric stretching band centered at 1076 cm^{-1} were both higher for Gram-positive bacteria (1076.13±0.53; 0.45±0.13) than for Gram-negative bacteria (1075.86±1.91;0.39±0.02) ($p<0.05$), (Fig. 4 and Table 2S†). Although the phosphodiester-related bands are quite prominent in the spectra of Gram-positive bacteria, it has been observed that Gram-negative bacteria contain a higher amount of phospholipids in their cell walls.[16,32] This demonstrates that the phosphate related bands of the FTIR spectra of Gram-positive than Gram-negative bacteria contain significant contributions from vibrations of phosphodiester groups unrelated to phospholipids. This is consistent with the fact that the cell wall and peptidoglycan layer of *Escherichia coli* are thinner (4 nm) than those of *Staphylococcus aureus* (50 nm). However, the presence of certain chemical moieties can be an indication of the spectrum of Gram-negative bacteria.[32, 33] The change in the DNA/protein content of the cells is frequently depicted by the peak area ratio of the bands (υPO_2 symmetric/Amide II),[32] applying this relationship in this case, FWHM ratio of bands (A_{1076}/A_{1539}). The result for Gram-positive bacteria (1.09±0.08) higher than Gram-negative bacteria (0.78±0.14) ($p<0.01$) (Table 1S†), indicating higher cellular DNA content in Gram-positive bacteria, which is consistent with previously reported bacterial species from research.[31,34] In addition, the FTIR spectra and their second derivatives (Fig. 4) also demonstrate a distinct difference in the chemical composition, including carbohydrate and phosphodiester groups of the cell wall, higher intensity and thicker cell wall in Gram-positive bacteria compared to low intensity and thinner cell wall in Gram-negative bacteria as they are more probably to rupture, which is consistent with other literature reports.[16,33,35] *Salmonella spp*. and *Bacillus subtilis* are the only Gram-positive and Gram-negative to exhibit the bands centered at 934 cm^{-1}, which are associated to the P-O-C stretching vibration and C-O-C ring deoxyribose, respectively.[22,27] Gram-negative bacteria including *Escherichia coli* has a thinner cell wall increasing the contribution of signal from cytoplasmic components such as DNA. Gram-positive and Gram-negative bacteria exhibit low intensity bands that are centered at 835 cm^{-1}, 746 cm^{-1}, 662 cm^{-1}, and 568 cm^{-1}, respectively. These low-intensity bands have a greater contribution of signals from components of the cell wall and cytoplasm. These include the aromatic ring vibrations of several nucleotides and nucleic acids, including phenylalanine, tyrosine, and triptophane; the C-H rocking of $>CH_2$ in proteins and fatty acids; aromatic bending rings of tyrosine (skeletal), guanine, and bases of DNA and RNA. [16,30,31] The FTIR spectrum of Gram-positive bacteria shows a significantly higher contribution from cell wall signals compared to the Gram-negative species used in this study.

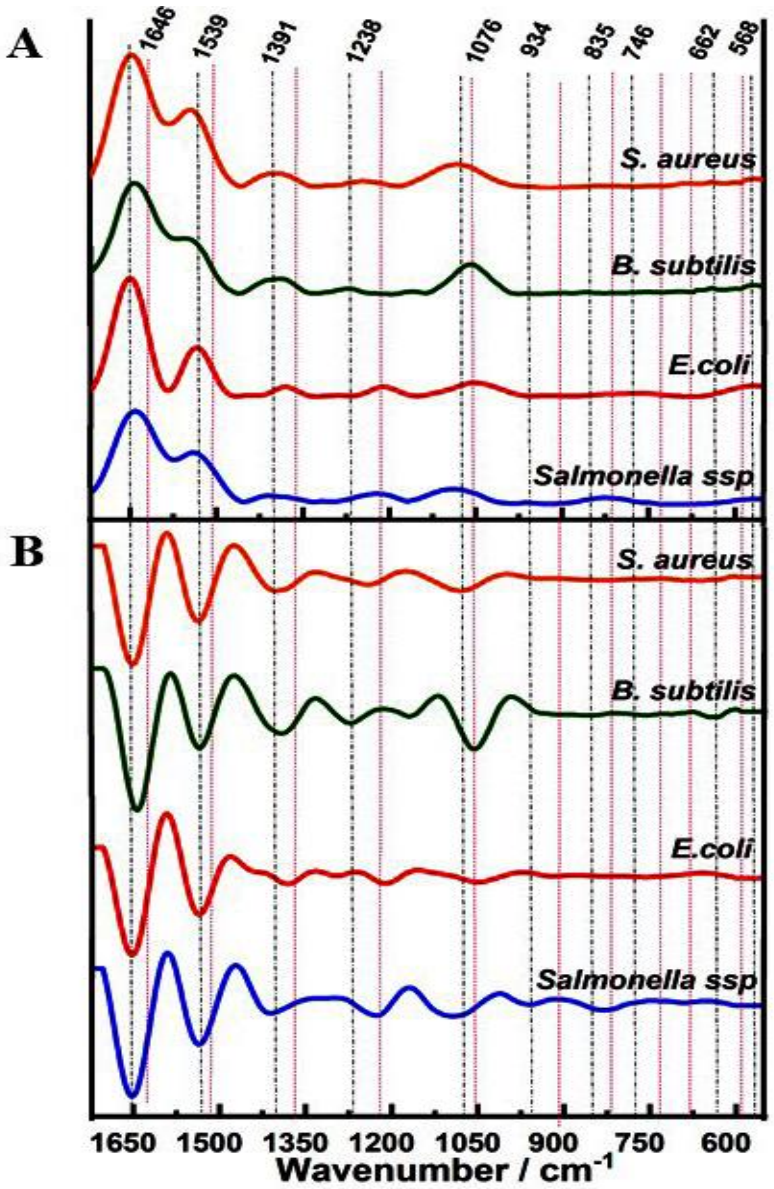

Fig. 4: A. Average FTIR spectra and, B. their second derivatives from top to the bottom collected from each bacterial strain analyzed in this study. Each FTIR spectrum was averaged from 18 tests recorded on random location on the same sample. All FTIR spectra were baseline corrected, normalized and shifted vertically for improved visualization. The plots are offset for clarity.

Reproducibility

The identification of pathogenic bacteria via FTIR spectroscopy demands rigorous cultivation and precise sample preparation to optimize **analytical turnaround time, detection limits, sensitivity, and reproducibility (Fig. 4)**. When coupled with principal component analysis (**PCA**), FTIR spectroscopy can effectively discriminate bacterial species, including phenotypic differentiation between **Gram-positive** and **Gram-negative** cohorts. Because the resulting FTIR spectrum captures the total biomolecular composition of cellular structures—including the cell wall, cytoplasm, and nucleic acids—robust spectral preprocessing is essential. Spectral quality must be systematically validated based on

absolute absorbance thresholds, **signal-to-noise ratios (SNR)**, and technical reproducibility. Consequently, preprocessing pipelines utilize the **Savitzky-Golay algorithm** to compute second derivatives, smooth spectral noise, and normalize data. Overall, PCA serves as a robust multivariate tool to verify measurement reproducibility and evaluate the clustering and overall separation of distinct bacterial cohorts. [20,26] To assess the reproducibility of the infrared signals, we acquired a total of twelve infrared spectra from four separate samples, collecting data from three randomly selected locations per sample. The FTIR spectral data for each sample were examined, and four prominent peaks (1076, 1391, 1539, and 1650 cm^{-1}) were selected to calculate the relative standard deviations (RSD) and evaluate measurement reproducibility (Fig. 3). For instance, high reproducibility of the FTIR spectra was observed at the prominent peak centered at 1646 cm^{-1}: *Staphylococcus aureus* and *Escherichia coli* (< 2.6%) and for *Bacillus subtilis* (14.0%) and *Salmonella spp.* (< 12%). However, the RSDs values increased (17%> RSD> 11%) for the peak centered at 1539 cm^{-1}, followed by the peak at 1391 cm^{-1} (15.6<RSDs <18.8%), then for the peak at 1076 cm^{-1} (12.5 <RSDs <20%), indicating that the reproducibility for the four bacterial species gradually changed within these limits. Although it has been reported in the literature that RSDs 20% variability are acceptable for quantitative studies using spectroscopic methods, the need for enhanced reproducibility of infrared spectra is continually increasing.[22]

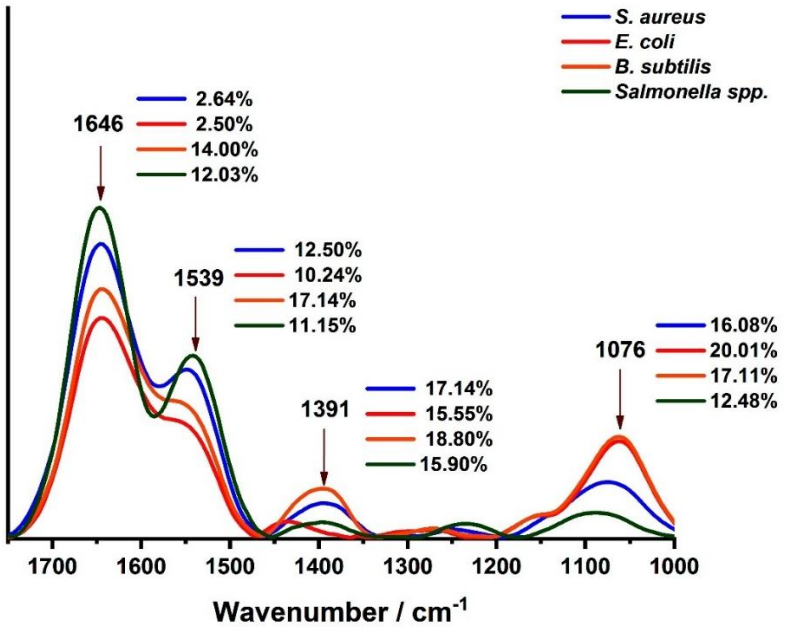

Fig. 4: Reproducibility of selected band intensities centered at: 1646, 1539, 1391 and 1076 cm^{-1} in the average FTIR spectra of: *S.aureus*, *B.subtilis*, *E.coli* and *Salmonella spp*.

Statistical Classification

The PCA analysis was first carried out for all the examined bacterial pathogens, including *Staphylococcus aureus*, *Escherichia coli*, *Bacillus subtilis*, and *Salmonella spp.*, in the whole wavelength range between 4000 and 550 cm^{-1}. In the first step we found that the three principal components (PCs)- PC-1, PC-2, and PC-3 explain 72.7%, 23.4%, and 3.6% of the variance in the data set studied (Fig. 5). Gram-positive and Gram-negative clusters separate along PC1, however there is not a distinct separation between bacterial species along PC2.

Gram-negative (*Escherichia coli* and *Salmonella spp.*) bacteria were clustered on the positive side of the PC-1 and PC-2 axis, forming a scattered and rather diffuse cluster (Fig. 5a), and Gram-positive (*Staphylococcus aureus* and *Bacillus subtilis*) bacteria were clustered on the negative side of PC-1 and the negative side of PC-2, forming a spread cluster, that makes it difficult to distinguish separately (Fig. 5b). Interestingly, PCA scores from FTIR of *Staphylococcus aureus* exhibited higher reproducibility because the scores of *Staphylococcus aureus.*were grouped more tightly pattern than *B.subtilis*. In addition, comparing *Staphylococcus aureus* scores to those of the other species, such as *Bacillus subtilis*, *Salmonella spp*. and *Escherichia coli*, whose scores were more randomly distributed and therefore, less reproducible corresponding to the RSD values determined for the four major band intensities of each specie (Fig. 2). Although, it was possible to recognize a pattern in the distribution of FTIR scores, *Escherichia coli* and *Salmonella spp*. were arranged in a more randomly pattern than *Staphylococcus aureus.* and *Bacillus subtilis* bacteria. Because it affects the distance between the scores for the same specie of bacteria and contributes to far-off clustering patterns because it impacts the distance between scores of different species. Unfortunately, in the whole spectra region PCA was unable to identify any distinct clustering among the four diverse bacterial species.[14,19]

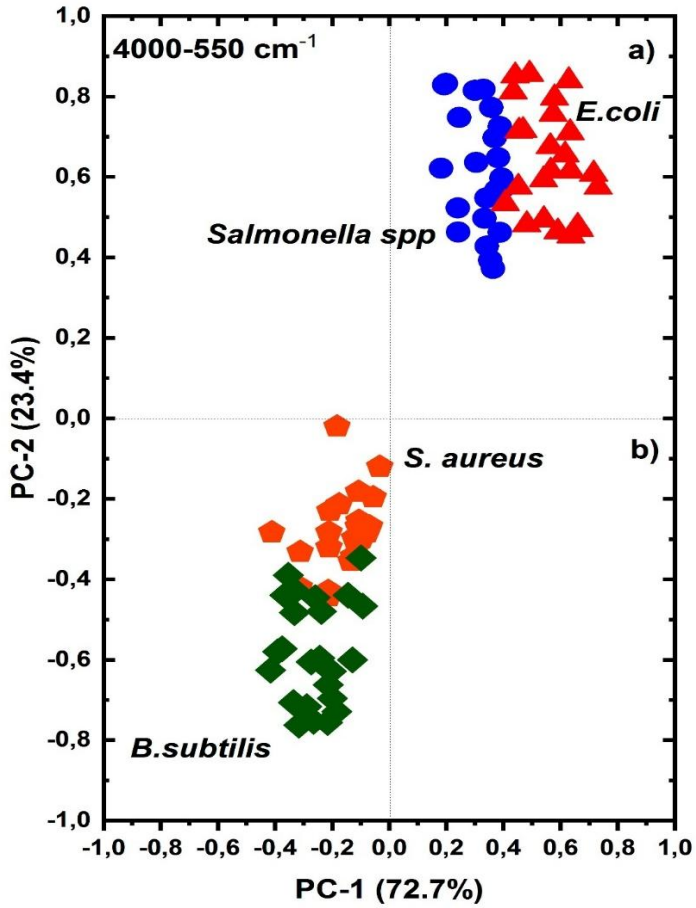

Fig. 5: Score plot of the first two principal components after PCA performed on FTIR spectra recorded from a) gram-negative: *E. coli* and *Salmonella spp*. and b) gram-positive: *S. aureus* and *B. subtilis* in the 4000-550 cm^{-1} region. The individual data points have been colour coded according to the results of cluster analysis.

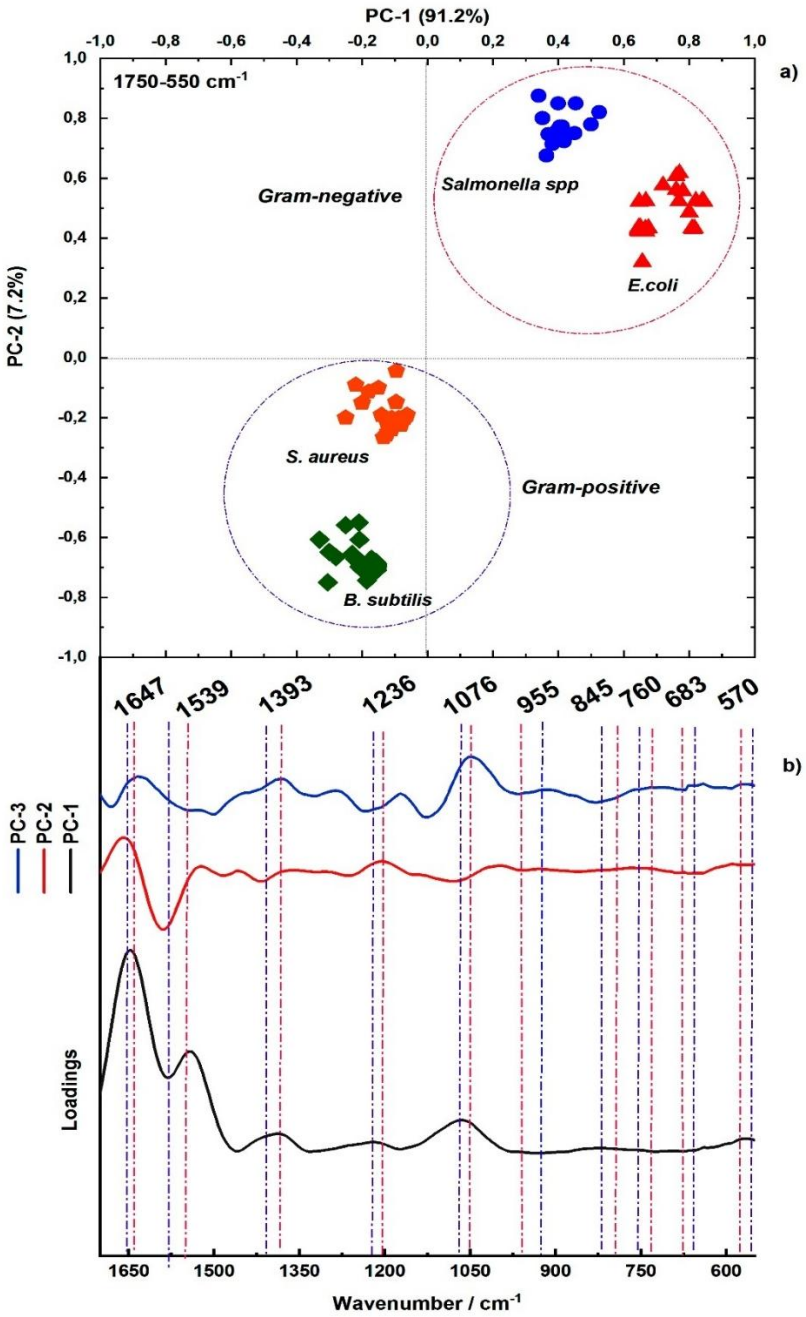

Fig. 6: a) First two principal components PCs (PC-1 and PC-2) scores plot of FTIR data calculated for the region 1700-550 cm^{-1}. The same strains are plotted in the same colours. b) PCA loadings associated to PC-1, PC-2 and PC-3 highlighting regions associated with large loadings for the same region.

In order to better identification among the four types of bacteria and to distinguish between Gram-positive and Gram-negative bacteria, PCA analysis was performed within a limited spectral region 1700-550 cm^{-1}, where the most important FTIR markers are present. Fig. 6 shows the PCA results and loading plots of the FTIR spectra of all the bacteria studied. In addition, Fig.6a shows the scores plot of the first two principal components PC-1 (91.2%) and PC-2 (7.2%) whose values each account for 98.4% of the total variance in the data set.

Interestingly, despite some variation in the PCA values from the same specie, the FTIR values in the limited region showed higher reproducibility because the values of each specie clustered closely together compared to the FTIR values of the full spectra, supporting the ability of FTIR to probe inter-individual variations in bacterial metabolism.[16,30] This demonstrates the remarkable division of the investigated bacteria into four distinct clusters, which correspond to the *Staphylococcus aureus*, *B.subtilis*, *E.coli*, and *Salmonella spp.*, respectively. According to the loading plots, the four bacterial species differ from each other based on the bands carefully examined in section 3.1 (Fig. 6b). The loadings provide information on the variables (spectrum wavenumber) essential for group discrimination. High loading values for variables are essential for diagnostic purposes. Unlike the FTIR spectrum, the loading spectrum has positive and negative bands, and their associated frequencies can be correlated with some of the most notable variations in the molecular composition of each bacteria under study (Fig. S2†). According to the FTIR spectra analysis and loading plots from PC-1 (PC-2 and PC-3), the most significant variation among these four bacteria: *Staphylococcus aureus*, *B.subtilis*, *E.coli*, and *Salmonella spp.* was found to be correlated with prominent bands centered at: 1076, 1238, 1391, 1539, 1646 cm^{-1}, as well as additional low intensitybands centered at 934, and 1744 cm^{-1}. These bands are associated with vibrational modes related to the compounds of bacterial cell walls such as, lipo-polysaccharides, lipoproteins and phospholipids, which enables the discrimination of Gram-positive from Gram-negative bacteria.[31,38]

CONCLUSIONS

Our study demonstrates that FTIR in combination with PCA is a powerful technique for the chemical characterization and differentiation of Gram-positive and Gram-negative pathogenic bacteria associated with foodborne diseases. In the spectral region between 2800 and 3300 cm^{-1}, we identified signals and ratios of representative biomolecules such as phospholipids and long-chain fatty acids, mainly derived from cell wall components. PCA of FTIR spectra in the region 1700-550 cm^{-1} showed high probability of discrimination between the four bacterial species clustered together between two Gram-positive (*Staphylococcus aureus.*and *Bacillus subtilis*) and two Gram-negative (*Escherichia coli* and *Salmonella spp.*) representatives, indicating a high probability of discrimination. In addition, the ratio of cellular DNA to protein and protein to lipids is significantly higher in Gram-positive bacteria than in Gram-negative bacteria due to differences in cell wall thickness. Moreover, spectroscopic signals of representative biomolecules at 1076, 1239, 1331, 1539, and 1640 cm^{-1} are related to compounds containing phosphodiesters (e.g., LTAs/TAs) and complex carbohydrates (e.g., peptidoglycan), which are primarily synthesized from components of the cell wall of each bacterial specie. Finally, foodborne pathogenic bacteria can be easily identified and reliably classified into Gram-positive and Gram-negative species with a high probability of data reproducibility using the FTIR approach and PCA analysis. This method can be applied to environmental biotechnology and food safety assessment.

Author Contributions

Conceptualization: experiments; data analysis; supervision; writing; review & editing: J.C. Ramirez Perez

Conflict of Interest

There are no conflicts to declare

Acknowledgements

The author gratefully acknowledges the support of the LNLS-CEPEM -University of Sao Paulo-Brazil for allowing us to use the microscopy FTIR Equipment for this research and thanks Prfa. Dra. Vania Melo Profa. Dra Vânia M.M. Melo, Universidade Federal do Ceará, Departamento de Biologia, Laboratório de Ecologia Microbiana e Biotecnologia (LemBiotech) Fortaleza-Ceará, Brasil for providing bacteria samples.

Funding: N/A

REFERENCES

1. CDC, 2020. Preliminary FoodNet data on the incidence of infection with pathogens transmitted commonly through food. https://www.cdc.gov/foodnet/reports/prelim-data-intro-2020.html. Accessed June 24
2. H. Yin-Yi, Y-T. Huang, D-F. Li, K-L Chen, Y. Chi, H-M, Tsai, H-W Cheng, J-K Wang, Y-L Wang, SERS-Based universal AST: Rapid treatment guidance for blood-culture bacteria before species identification, Anal Chem., 98 (2026), 5989-6002. DOI:10.1021/acs.analchem.5c04833
3. GRAMGlobal Research on Antimicrobial Resistance, Bacterial infections linked on eight global deaths, according GRAM study, Publication 22 Nov. (2022) https://www.tropicalmedicine.ox.ac.uk/Gram/
4. A.Samuels, D. Snyder, D. Emge, J. Amant, M. Minter, A. Campbell, Classification of select category A and B by FTIR, Applied spectroscopy, 63 (2009) 14-24.
5. Y Sadaie, K. Matsumoto, Escherichia coli, and Bacillus subtilis: the frontiers of molecular microbiology revisited, (2012), Thiruvananthapuram, Karla: Research signpost, 115-148
6. L.Gan, S. Chen, GJ Jenses, Molecualr organization of Gram-negative peptidoglycan, Proc. Natl. Acad. Sci. USA, 105 (2008),18953-18957. DOI:10.1073/pnas.0808035105
7. KC. Huang, R. Mukhopadhyay, B Wen, Z. Gitai, NS.Wingreen, Cell shape and cell-wall organization in Gram-negative bacteria, Proc. Natl. Acad. Sci. USA, 105 (2008),19282-19287. DOI:10.1073/pnas.0805309105
8. P. Feng, P, Rapid methods for detecting foodborne pathogens, Bacteriological Analytical Manual Online, FDA/Center for Food Safety and Applied Nutrition. http://www.cfsan.fda.gov/~ebam/bam-a1.html. Accessed 1 July.
9. D.Y.C. Fung, Rapid methods and automation in microbiology, Compr. Rev. Food Sci. Technol., 1 (2002) 3–22.
10. A. Alvarez-Ordonez, DJM. Mouwen, M. Lopez, M. Prieto, Review: Fourier transform spectroscopy as a tool to characterize molecular composition and stress response in foodborne pathogenic bacteria, Journal of Microbiological Methods, 84 (2011) 369-378.
11. J.C. Ramirez-Perez, T. Alves, M. Rizzutto, Impact of silver nanoparticles size on SERS detection and identification of filamentous fungi, Spectroschimica acta Part A: Molecular and Biomolecular Spectroscopy, 272 (2022), 120980. DOI:10.1016/j.saa.2022.120980

12. J.C. Ramirez-Perez, T. Alves dos Reis, M. Rizzutto, Identifying and detecting Entomopathogenic fungi using Surface-enhanced Raman spectroscopy, Brazilian Journal of Animal and Environmental Research, 4 (2021) 4832-4850. DOI:10.34188/bjaerv4n4-002

13. F. Wong, C. de la Fuente, J. Collins, Leveraging artificial intelligence in the fight against infectious diseases, Science, 15 (2023), 26398-26406

14. J.C. Ramirez-Perez and D. Durigo, Surface-enhanced raman spectroscopy (SERS) for characterization SARS-CoV-2, Journal of Saudi Chemical Society, 26 (2022), 101531. DOI:10.1016/jscs.2022.101531

15. D. Naumann, H.H. Mantsch, M. (Hrsg) Jackson (Eds.), Infrared and NIR Raman Spectroscopy in Medical Microbiology, Proceedings of SPIE Washington, Bellingham, 1998, pp. 245–257.

16. S. Efrima & L. Zeiri. Understanding SERS of Bacteria, J. Raman Spectros, 40 (2009) 277-288.

17. D. Naumann, FT-Infrared and FT-Raman spectroscopy in biomedical research, Appl. Spectrosc. Rev., 36 (2001) 239–298. DOI:10.1081/ASR-100106157

18. Y. Xie, S. Xu, Y. Hu, W. Chen, Y. He, X. Shi, Rapid identification and classification of *Staphyococcus aureus* by attenuated total reflectance Fourier Transform Infrared Spectroscopy. Journal of Food Safety, 32 (2012) 176-183.

19. E. Salman, U Shufan, I. Sharanda, S. Lapidot, M. Mordechai, Huleihel, Distiction between mixed species bacteria using infrared spectroscopy and multivariate analysis, Vibrational Spectroscopy, 100 (2019) 6-13.

20. Y. W., Bozhou Chen, G. Fang Zhang, C. Sheng, Rapid Broad-Spectrum Colorimetric Detection of Bacteria Using Polylysine-Mediated Gold Nanoparticle Aggregation. *Anal. Chem,* 98 (34) (2026) 24984–24992. DOI: 10.1021/acs.analchem.6c02521

21. L.X., Daian Chen, T.D., Ruiying Peng, L. Jishan, Proximity Singlet-Oxygen-Activation and Luminescence-Controllable Chemiluminescent Assay for Fast Ultrasensitive Detection of Pathogenic Bacteria. *Anal. Chem.* 98 (12) (2026), 9046–9053. DOI: 10.1021/acs.analchem.5c07323

22. S.Garip.F. Bozoglu, F. Severcan, Differentiation of mesophilic and thermophilic bacteria with Fourier Transform Infrared Spectroscopy, Applied Spectroscopy, 61 (2) (2007), 186-192.

23. S. Pahlow, S. Meisel, D. Cialla-May, K. Weber, P. Rösch, J. Popp, Isolation and identification of bacteria by means of Raman spectroscopy, Adv. Drug Deliv. Rev. 89 (2015) 105–120.

24. C. Lima, S. Ahmed, Y. Xu, H. Muhamadali, C. Parry, R.J McGalliard, E.D. Carrol, R. Goodacre, Simultaneous Raman and infrared spectroscopy:a novel combination for studying bacterial infections at the single cell level, Chem. Sci, 13 (2022) 8171-8179.

25. J. Kneipp, M.Beekes, P. Lash, and D. Naumann, Molecular changes of preclinical scrapie can be by infrared spectroscopy, J. Neurosci, 22 (2002) 2989-2997

26. C. Rebuffo, J. Schmitt, M. Wenning, F. von Stetten, S. Scherer, Reliable and rapid identification of Listeria monocytogenes and Listeria species by artificial neural netwoek-based Fourier transform infrared spectroscopy, Applied and Env. Microbiology, 72 (2) (2006), 994-1000

27. J. Hu, S. Xie, J. Fan, *et al.* Simple, Rapid, and Visual Detection of *Escherichia coli* O157 in Raw Milk by Recombinase Polymerase Amplification with Polymer Flocculation Sedimentation. Food Anal. Methods, 18 (2025)., 2542–2555. DOI:10.1007/s12161-025-02878-9

28. A. Melin, A. Perromat, G.Deleris, Pharmacologic application of Fourier transform IR spectroscopy: In vivo toxicity of carbon tetrachloride on rat liver, Biopolymers 57 (2000) , 160-168.

29. B.Szalontai, Y. Nishiyama, Z. Gombos, N. Murata, membrae dynamics as seen by FITR spectroscopy in a cyanobacterium, *Synechocystis* PCC6803:The effects of lipid unsaturation and the protein-to-lipid ratio, Biochim. Biophys, Acta 1509 (2000), 409-419

30. K.Kochan, D. Peres, J. Pissang, J-H Jiang, A. Peleg, D. McNaughton, P Heraud, B. R.Wood, In vivo atomic forcé microscopy-infrared spectroscopy of bacteria, J.R.Soc. Interface, 15 (2018) 20180115

31. A.Barth, Infrared spectroscopy of proteins, Biochim. and Biophys Acta, 1767(2007), 1073-1101.

32. W Jiang, A Saxena, B Song, B Ward, TJ Beveridge, SC Myneni, Elucidation of functional groups on Gram-positive and Gram-negative bacterial surfaces using infrared spectroscopy, Langmuir 20 (2004) 11433-11442

33. D. Naumann,,Some ultrastructural information on intact, living bacterial cells and related cell-wall fragments as given by FTIR, Infrared Phys, 24 (1984) 24, 233-238

34. A.A. Kamnev, FTIR spectroscopy studies of bacterial cellular responses to environmental factors, plant-bacterial interactions and signaling, Spectroscopy, 22 (2008), 83-95

35. JR. Mourant, YR. Yamada, S Carpented, LR. Dominique, JP. Freyer, FTIR spectroscopy demonstrates biochemical differences in mammalian cell cultures at different growth stages, Biophys. J, 85 (2003), 1938-1947

36. A. van Belkum, C. Burnham, J.W. Rossen, et al. Innovative and rapid antimicrobial susceptibility testing systems, Nat. Rev. Microbiol, 18 (2020), 299-311

37. R. A. Sakata, R. Cayo da Silva, A. Gales; et al. Broad spectrum antimicrobial consumption trends and correlation with bacterial infections and antimicrobial resistance over 5 years. J. Global Antimicrob. Resist. 28 (2022), 115-119

38. S.-Y Chiu, H. Cheng, Z. Chen, et al. Quantification of biomolecules responsible for biomarkers in the surface-enhanced Raman spectra of bacteria using liquid chromatography-mass spectrometry, Phys.Chem. Chem. Phys., 20 (2018), 8032-8041

SUPPLEMENTARY MATERIALS

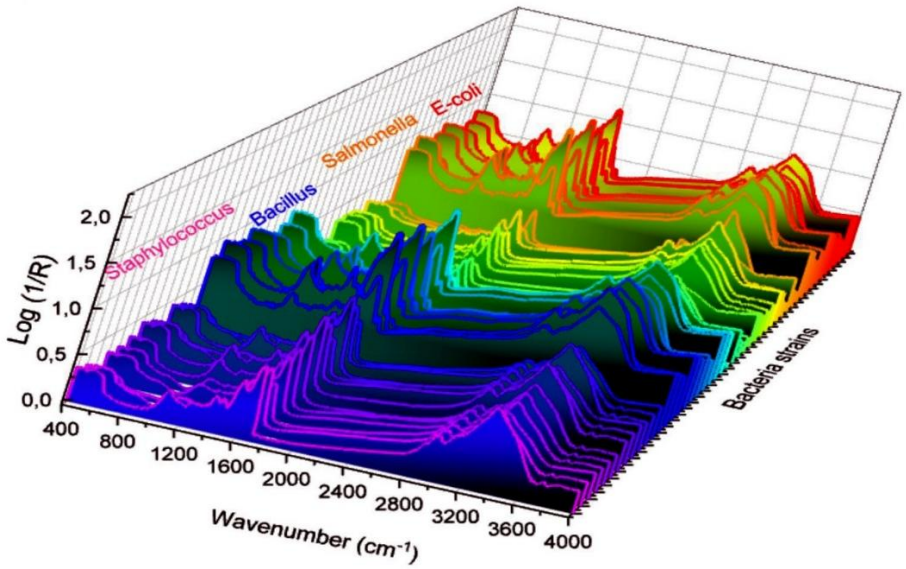

Fig. S1: 3D FTIR spectra image of four pathogenic bacteria: *Staphylococcus aureus*, *Bacillus subtilis*, *E.coli* and *Salmonella spp*. in the range 4000-400 cm^{-1}

Table S1: The band frequency and intensity and FWHM values of different functional groups in the Gram-positive and Gram-negative bacterial samples

				Frequency		
	Gram-positive			Gram-negative		
Functional groups	*S.aureus*	*B.subtilis*	Group Gram *(+)*	*E.coli*	*Salmonella spp.*	Group Gram *(-)*
CH_3 asymmetric stretching*	2971.47+/-0.14	2971.27+/-0.15	2971,37+/-0,15	2967.63+/-0.05	2970.98+/-0.04	2969,31+/-0,00
CH_2 asymmetric stretching*	2931.35+/-0.02	2927.55+/-0.02	2951,45+/-0,02	2925.60+/-0.04	2929.47+/-0.04	2927,54+/-0,04
CH_3 symmetric stretching*	2872.03+/-0.14	2867.98+/-0.15	2870,01+/-0,15	2868.00+/-0.00	2881.25+/-0.03	2874,63+/-0,02
CH_2 symmetric stretching*	2852.33+/-0.03	2850.35+/-0.04	2851,34+/-0,04	2850.27+/-0.04	2852.21+/-0.01	2851,24+/-0,03
Amide I*	1644.57+/-0.77	1643.42+/-1.24	1644,00+/-1,00	1645.45+/-1.31	1647.90+/-1.10	1646,68+/-0,1,21
Amide II*	1539.25+/-0.51	1537.41+/-1.07	1538,33+/-0,79	1539.41+/-1.11	1537.81+/-0.59	1538,61+/-0,85
COO symmetric stretching*	1387.65+/-0.73	1398.00+/-0.26	1392,83+/-0,49	1382.64+/-0.17	1394.28+/-0.67	1388,46+/-0,42
PO_2 asymmetric stretching*	1233.30+/-0.85	1244.14+/-0.21	1238,72+/-0,51	1242.26+/-0.07	1230.72+/-2.00	1236,49+/-1,35
PO_2 symmetric stretching*	1092.31+/-1.78	1059.95+/-0.74	1076,13+/-0,53	1059.92+/-0.75	1091.79+/-3.17	1075,86+/-1,96

			Intensity			
	Gram-positive			Gram-negative		
Functional groups	***S.aureus***	***B.subtilis***	**Group Gram (+)**	***E.coli***	***Salmonella spp.***	**Group Gram (-)**
CH_3 asymmetric stretching*	0.49+/-0.05	0.49+/-0.10	0,49+/-0,07	0.79+/-0.13	0.63+/-0.18	0,71+/-0,15
CH_2 asymmetric stretching*	0.47+/-0.05	0.50+/-0.10	0,49+/-0,07	0.77+/-0.13	0.75+/-0.20	0,76+/-0,16
CH_3 symmetric stretching*	0.40+/-0.05	0.41+/-0.09	0,41+/-0,07	0.71+/-0.11	0.74+/-0.20	0,73+/-0,15
CH_2 symmetric stretching*	0.37+/-0.04	0.40+/-0.09	0,39+/-0,65	0.64+/-0.11	0.66+/-0.19	0,65+/-0,15
Amide I*	0.71+/-0.15	0.99+/-0.28	0,85+/-0,21	0.99+/-0.27	0.40+/-0.10	0,70+/-0,18
Amide II*	0.54+/-0.13	0.82+/-0.25	0,68+/-0,19	0.82+/-0.25	0.30+/-0.09	0,56+/-0,17
COO symmetric stretching*	0.30+/-0.09	0.65+/-0.18	0,48+/-0,85	0.52+/-0.11	0.15+/-0.06	0,34+/-0,08
PO_2 asymmetric stretching*	0.19+/-0.08	0.51+/-0.11	0,35+/-0,02	0.51+/-0.10	0.11+/-0.05	0,31+/-0,07
PO_2 symmetric stretching*	0.23+/-0.10	0.67+/-0.17	0,45+/-0,13	0.69+/-0.18	0.09+/-0.01	0,39+/-0,02

				FWHM		
	Gram-positive			Gram-negative		
Functional groups	***S.aureus***	***B.subtilis***	**Group Gram (+)**	***E.coli***	***Salmonella spp.***	**Group Gram (-)**
CH_3 asymmetric stretching*	220.53+/-31.37	217.27+/-46.11	218,90+/-38,74	127.83+/-19.34	147.87+/-39.99	137,86+/-29.5
CH_2 asymmetric stretching*	331.24+/-82.98	251.30+/-77.20	291,27+/-80,00	389.55+/-33.21	346.85+/-20.74	368,20+/-26.98
CH_3 symmetric stretching*	285.66+/-23.78	284.58+/-2.65	285,12+/-13.21	231.70+/-23.04	201.30+/-49.13	216,5+/-36.08
CH_2 symmetric stretching*	283.68+/-3.42	506.64+/-53.27	395,16+/-28,34	578.06+/-38.00	668.91+/-36.53	623,43+/-37.27
Amide I*	93.90+/-2.34	117.81+/-8.67	105,86+/-5.50	116.83+/-9.97	92.13+/-1.25	104,48+/-5.61
Amide II*	143.20+/-12.76	651.65+/-18.55	397,43+/-15.65	681.16+/-16.56	117.05+/-1.85	399,11+/-9.21
COO symmetric stretching*	194.43+/-25.76	154.05+/-47.46	174,24+/-36,61	224.14+/-9.18	165.17+/-4.17	194,66+/-6.68
PO_2 asymmetric stretching*	195.03+/-42.21	432.84+/-19.57	313,94+/-30.89	298.50+/-14.17	144.47+/-3.92	221,49+/-9.05
PO_2 symmetric stretching*	257.64+/-64.00	245.62+/-41.04	251,63+/-52.52	171.98+/-10.03	152.62+/-7.13	162,30+/-8.58
* p<0,05						

Table S2: The band FWHM ratios of some functional groups in the Gram-positive and Gram-negative bacterial samples

Ratio of FWHM of peaks	Functional groups	Gram-positive			Gram-negative		
		S.aureus	***B.subtilis***	**Ave Gram (+) species**	***E.coli***	***Salmonella spp.***	**Ave Gram (-) species**
Protein/lipid**	Amide I + Amide II/CH3 sym.+ CH3 asym.+ CH2 sym + CH2 asym.	0.21+/-0.04	0.61+/-0.03	0.41+/-0.04	0.60+/-0.02	0.15+/-0.03	0.38+/-0.03
DNA/protein**	PO2 symmetric/Amide II	1.80+/-0.07	0.38+/-0.08	1.09+/-0.08	0.25+/-0.06	1.30+/-0.02	0.78+/-0.04
**p<0,01							

Principal Component Analysis

The principal component analysis (PCA) is a dimensionally-reduction method that is often used to reduce the dimensionality of large data sets, by transforming a large data set of variables into smaller one, called principal components (PC) that still contains most of the information in the larger set. The first principal component (PC-1) accounts for the greatest variability in the data as possible. The method of PCA is based on a model assuming $X = TP^T + E$, where the X matrix is decomposed by PCA into two smaller matrices, one of scores (T) and other of loadings P^*, and E is the error matrix. PC's scores are related to a linear combination of the original variables, and describe the differences or similarities in the

sample (plots of PC-1 vs PC-2). PCA provides insight into the percentage of variance explained by each PC and shows how many PCs should be kept to maintain the maximum information from the original data without adding noise to the current information. Loadings describe the data structure in terms of variable correlation and reflect how well PC takes into account the variation of that variable. By analysing the plot of PC-loadings as a function of the variables (i.e. wavenumber) one can indicate the most important diagnostic variables or regions related to the differences found in the data set (Fig. 2S).

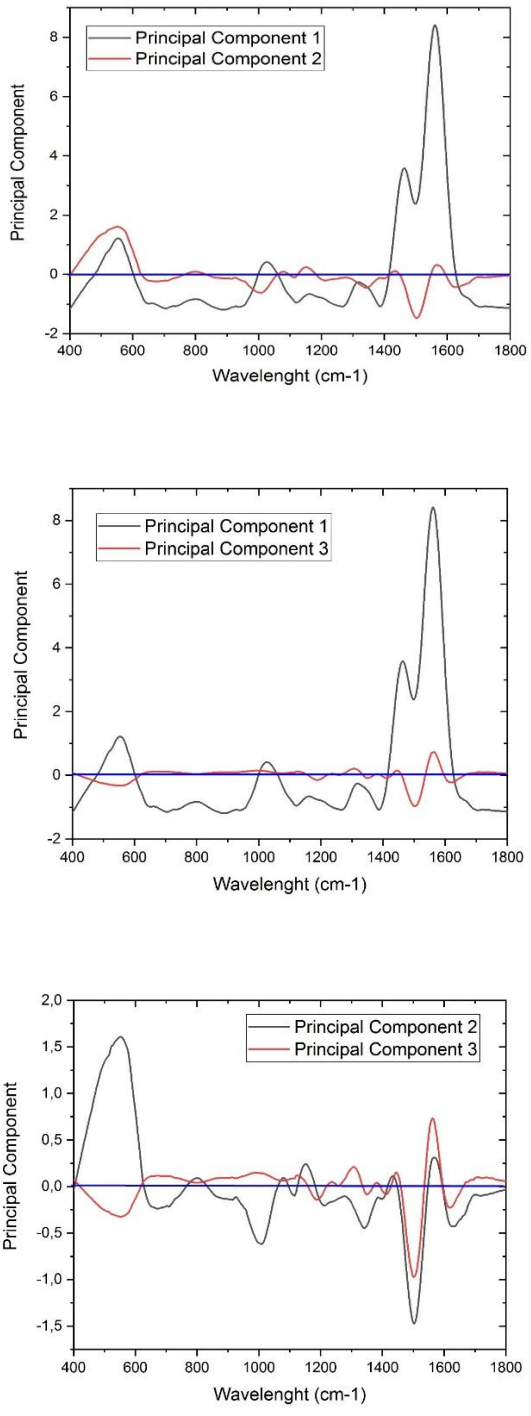

Fig.2S: Loadings plots of the first principal components PC-1 to PC-3 for the investigated Raman spectral region * Cowe, I., McNicol J. 1985.